International Journal of Scientific Engineering and Science
Volume 10, Issue 7, pp. 20-24, July 2026. ISSN (Online): 2456-7361

Selection of Textile Material for Impact Absorption Shoe Attachment of Skydiver

S.J.S. Sewmini, P.A.S. Dasunika, S.P.M. Silva, P.L. Liyanage, S.N. Niles, K.P.M.C.K.B. Karunaratne, T.S.S. Jayawardane, E.A.S.K. Fernando
Department of Textile and Apparel Engineering, University of Moratuwa, Moratuwa, Sri Lanka

***Abstract*— *Skydiving popularized as an extreme sport as well as military practice and safe landing of skydivers become greater importance. Deviation from perfect landing may result in leg injuries of skydivers and a system to prevent such leg injuries is critical. So, the development of impact absorption systems for skydivers, aimed at reducing the force applied to the feet during high-speed imperfect landings. This paper focuses on analyzing the skydiver's motion in landing and the selection of textile materials for the shoe attachment to absorb the impact force during high-speed descent. Further, several tests were carried out to ensure the conformity of material performance for shock absorbency component of the shoe based on the calculations of skydiver's motion analysis. Five different fabric types, composed of PA66 and PET, were tested to evaluate their air permeability, bursting strength, breaking strength, and tearing strength. The findings of this research provide a foundation for designing an effective impact absorption attachment for skydivers, aiming to minimize the impact forces experienced by the skydivers.*

***Keywords*— *Impact absorption, Safe landing, Fabric selection and testing, Shoe attachment*

I. Introduction

Skydiving is a non-motorized extreme sport undertaken for both recreational and military purposes. Among the various risks involved, lower limb injuries are particularly prevalent, accounting for approximately 51% of all injuries sustained by skydivers [1]. Among them, 83–90% of these injuries occur during the landing phase [1], with high-speed landings emerging as a major global cause of skydiving-related injuries [2]. During these landings, high-speed contact with the ground can generate substantial compressive forces. If these forces exceed the biomechanical tolerance limits of skeletal structures, fractures are likely to occur. The reported tolerance thresholds are approximately 6.75 kN for the ankle, 10 kN for the femur, and 9.5 kN for the pelvis [3].

Skydivers commonly use standard running shoes during landings. However, studies have shown that amateur skydivers experience average ground reaction forces of approximately 4.38kN during landing, which approaches the injury threshold for the ankle (6.75 kN) [4]. Conventional running shoes can absorb only about 12.7% of the total impact force (approximately 689.92 N) [5], which is inadequate for protecting against the high loads experienced during high-speed landings. In response to this challenge, several innovative solutions have been proposed found in patents, including airbag-based shoe soles [6] and military-grade boots equipped with surface-expanding systems using pressure recoil mechanisms [7].

Among the proposed solutions for mitigating landing impact, an airbag-based shoe sole for paratroopers features a dual-airbag sandwich structure positioned at the front and rear of the sole. These airbags are filled with flexible foam and connected to atmospheric air valves. Before landing, the airbags inflate, and upon ground contact, air is released through the valves to dissipate impact energy [6]. Another patented design, a military boot with a surface-expanding system employing a pressure recoil mechanism, used a combination of inflatable air chambers, a wax-sealed water reservoir, and layered materials to enhance shock absorption. In this system, an electric inflator pump pre-fills the air chambers, while a sensing mechanism triggers the release of water upon landing. The ejected water generates a recoil effect that opposes the landing force, contributing to further impact reduction [7].

Despite their innovative concepts, these patents do not quantify the actual reduction in impact force achieved by each system. Therefore, there is a need for a validated solution that effectively absorbs the forces experienced during high-speed landings. To absorb this impact force, a fabric-based air component with controlled fabric properties can be used.

The impact reduction principle is used in car airbags, where a cushioning effect reduces the force on the human body by extending the duration of collision. Inspired by this mechanism, a fabric component for a shoe can be designed to enhance the collision time by controlling the air permeability of the fabric. A careful selection of the appropriate textile materials based on their technical properties to meet the expected level of shock absorbency through scientific calculation of skydivers' motion was carried out.

II. Vertical Motion Analysis Of Skydivers

The motion of a skydiver can be analyzed using the velocity-time graph shown in Fig. 1, which illustrates four distinct phases. In Phase 1, the skydiver jumps from the aircraft and accelerates under the influence of gravity. This acceleration continues until the skydiver reaches a constant velocity in Phase 2, known as the terminal velocity, approximately 60 m/s [8]. While descending at this terminal velocity, the skydiver deploys the parachute at an altitude of 3000 meters above the ground [8]. The deployment significantly increases the surface area exposed to air, thereby increasing air resistance. As a result, in Phase 3, the skydiver undergoes rapid deceleration. After a short period of deceleration, the skydiver enters Phase 4, where a new, lower terminal velocity is reached and maintained until landing.

International Journal of Scientific Engineering and Science
Volume 10, Issue 7, pp. 20-24, July 2026. ISSN (Online): 2456-7361

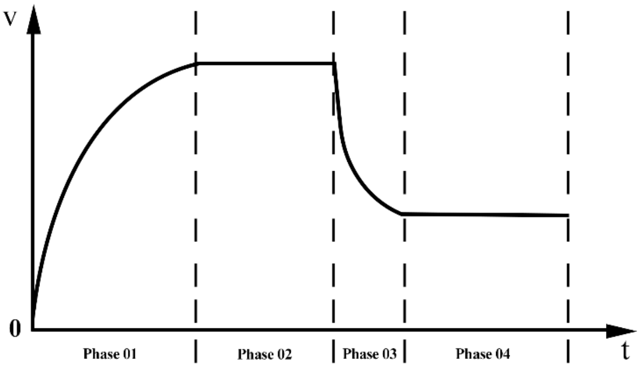

Fig. 1. Velocity-time graph of the vertical motion of a skydiver

During the derivation of the velocity equation, m, ρ and g represent the mass of the skydiver, the density of air, and the acceleration due to gravity respectively. In Phases 1 and 2, the skydiver without the parachute is considered as the parachute is yet to be deployed. However, in Phases 3 and 4, both the skydiver and the parachute must be taken into account, as the parachute is already deployed at the end of Phase 2. Therefore, in two latter phases, the effective cross-sectional area (A) and drag coefficient (C_d) are considered based on the combined effect of the parachute and skydiver.

In Phase 1, the skydiver begins the motion from rest. Accordingly, the velocity equation can be derived from Newton's second law, incorporating the drag force experienced by the skydiver. At this stage, the drag force is calculated using the frontal area (A) and the drag coefficient (C_d) corresponding to the skydiver's body alone. By applying Newton's second law of motion, the drag force F_D can be stated as follows.

$$mg - F_D = ma_1 \quad (1)$$

$$F_D = m(g - a_1) \quad (2)$$

By substitution for the drag force in equation (1) the following equation could be yielded.

$$0.5\rho C_d A V_1^2 = m(g - a_1) \quad (3)$$

Substituting $a_1 = \frac{dV_1}{dt}$, in equation (2) dynamic differential equation describing the variation of velocity with time in Phase 1 was obtained and solution to this differential equation is given as.

$$V_1 = \sqrt{\frac{2mg}{\rho A C_d}} \coth\left(t\sqrt{\frac{\rho C_d A g}{2m}}\right) \quad (4)$$

In Phase 2, the skydiver reaches a constant velocity as the upward drag force balances the downward gravitational force. This equilibrium conditions can be stated as

$$F_D = mg \quad (5)$$

Substituting for drag force equation (5) could be derived.

$$0.5\rho C_d A V_2^2 = mg \quad (6)$$

Where V_2 is the terminal velocity achieved only with skydiver. So, V_2 can be expressed as.

$$V_2 = \sqrt{\frac{2mg}{\rho C_d A}} \quad (7)$$

Similar to Phase 1, the velocity equation for Phase 3 can be derived using Newton's second law, as shown below. However, unlike Phase 1, the initial conditions are not zero since the skydiver is already in motion when the parachute is deployed. In this derivation, the increased cross-sectional area of the parachute (A_p) and the corresponding drag coefficient (C_{dp}) are considered to model the increased air resistance.

$$V_3 = \sqrt{\frac{2mg}{\rho A_p C_{dp}}} \tanh\left(t\sqrt{\frac{\rho A_p C_{dp} g}{2m}}\right) \quad (8)$$

Similar in phase 02, the terminal velocity V_4 with parachute in phase 04 can be derived as below.

$$V_4 = \sqrt{\frac{2mg}{\rho C_{dp} A_p}} \quad (9)$$

III. Selection of Material and Testing

A. Proposed Design

Fig. 2. Components of the proposed design

The proposed design comprises three main components, as illustrated in Fig. 2: the fixing insole, the woven midsole, and the outsole. The fixing insole serves as the interface for securely attaching the product to the interior of the shoe. The outsole functions as the primary contact surface with the ground.

Based on the literature, thermoplastic polyurethane (TPU) was selected as the material for both the fixing sole and outsole due to its durability, abrasion resistance, flexibility, and compatibility with 3D printing for prototyping purposes[9].

The woven midsole is the key component responsible for absorbing impact forces and mitigating them through the air permeability of the fabric. Upon ground contact, the midsole undergoes controlled compression, during which the porous structure of the woven material enables a gradual release of air. This controlled air release prolongs the duration of impact, thereby reducing the peak force transmitted to the skydiver. According to existing literature, compressed CO_2 is selected over N_2 for inflating the midsole component, as CO_2 can generate higher pressures using a smaller volume of gas, enhancing the overall efficiency of the system [10].

The system is activated through real-time monitoring of altitude and acceleration, using barometric and MPU sensors [11], [12]. Upon detecting the appropriate threshold, the mechanism releases compressed CO_2 from the air canister, initiating the midsole component within 0.5 seconds prior to ground contact. Therefore, the air permeability level of the selected midsole fabric must be carefully optimized to ensure proper inflation timing and effective impact mitigation.

IV. Fabric Selection For Woven Midsole Component

A. Development of Fabric Specifications According to The Requirement

Airbag fabrics are characterized by a bursting strength exceeding 1500 kPa and an air permeability of approximately 3.1 L/min [11], [12], which are critical parameters for ensuring both durability and controlled inflation performance in safety applications. Consequently, these key parameters, namely bursting strength and air permeability were determined using the aforesaid mathematical equations derived.

The required bursting strength was determined by referencing the maximum force at which a lower limb bone fractures, which is 10 kN [3]. Therefore, the fabric must be capable of withstanding a force of 10 kN. In addition, since skydivers experience forces arising from both body weight and impact during landing, the fabric's bursting strength must withstand the resultant force from these combined effects. The calculations were done based on a maximum skydiver weight of 114 kg [13], and the standard foot area taken as UK size 10. By the definition of pressure, the maximum pressure that can be exerted on one foot can be expressed as follows.

$$P = \frac{10{,}000 + 114 \times 9.81}{0.0319} = 348{,}537\ Pa \qquad (10)$$

To ensure compatibility with the application, the required air permeability was determined by analyzing the volume of air released during the complete inflation period (0.5 seconds) of the component, which resulted in a value of 1.6 L/min.

The number of air molecules released during the inflation time, n_a, is determined by considering the number of air molecules released to the component during inflation, n_{in}, and the number of air molecules that should be retained until ground contact, n.

$$n_a = n_{in} - n \qquad (11)$$

The number of air molecules released to the component during inflation time, (n_{in}) is determined by considering the rate of air release to the component, (Q_{in}) over-inflation time, (t) as follows.

The volume can be expressed as the mass divided by the density.

$$Q_{in} = \frac{vol}{t} \qquad (12)$$

To find Q_{in}Determine the volume of air released to the component using the density relationship:

$$vol = \frac{m_{in}}{\rho} \qquad (13)$$

From the mole formula, the mass of air released to the component can be determined.

$$n_{in} = \frac{m_{in}}{M} \qquad (14)$$

Where M is the molecular weight of the inlet air. By substituting for equation (11) from equation (12), and (13), the rate of air release to the component during inflation time t can be expressed as,

$$Q_{in} = \frac{n_{in} M}{\rho t} \qquad (15)$$

So, equation (14) can be arranged to express n_{in} as follows.

$$n_{in} = \frac{Q_{in} \rho t}{M} \qquad (16)$$

From the real gas equation, the number of air molecules that should be retained until ground contact, n can be found. So, the air permeability of the fabric Q is determined by the equation (16).

$$Q = \frac{n_a M}{\rho t} \qquad (17)$$

B. Reference Fabric Specifications

Based on the above calculated benchmark values and the fabric specifications for the commercially available vehicle airbags, the following fabric specifications have been derived as given in Table I to fulfill the specific requirements [13], [14].

TABLE I. Fabric specifications

Property		Value	Value
Fiber Type		PA66	PET
Weave		Plain	Plain
Silicone Coating		Coated	Coated
EPI		44	58
PPI		42	48
Thickness (mm)		0.44	0.58
Fabric GSM		240	345
Breaking Strength (N)	Warp	2563	2078
	Weft	2505	2008
Tearing Strength (N)	Warp	526.74	284
	Weft	505.4	278
Bursting Strength kPa		>348.5	>348.5
Air Permeability (L/min)		1.6	1.6
Elongation (%)	Warp	23.5	14.89
	Weft	21.3	14.9

C. Selection Procedure of The Fabric For The Requirement

In accordance with the developed fabric specifications as given in Table I, five fabric samples were sourced as shown in Table II.

TABLE II. Fabric specifications of the tested samples

Property	Sample A	Sample B	Sample C	Sample D	Sample E
Fiber Type	PA66	PA66	PET	PA66	PA66
Weave	Plain	Plain	Plain	Ripstop	Ripstop
Silicone Coating	Coated	Coated	Not Coated	Not Coated	Not Coated
EPI	45	44	77	76	68
PPI	42	40	36	54	52
Thickness (mm)	0.3	0.3	0.2	0.2	0.1
Fabric GSM	208.13	215.05	114.36	70	32

The tests have been carried out using the test standards given below [15]. To select the most suitable fabric based on the requirements outlined in the specifications.

- Air permeability test (ASTM D 737-96)
- Bursting strength test (ASTM D 3786-18)
- Tearing strength test (ASTM D 2261)
- Tensile strength test (ASTM D 5034)

V. Results and Discussion

The five samples, namely A, B, C, D, and E were tested for air permeability, bursting strength, tearing strength and tensile strength warp-way and weft-way. The results were depicted in Fig. 3 through Fig. 6.

As shown in Fig. 3, samples A, B, and C recorded air permeability values above the minimum requirement, with Sample C showing the highest permeability at approximately 6.6 L/min. In contrast, Samples D and E demonstrated negligible air permeability (~0.02 L/min), significantly below the threshold. The high air permeability of Sample C may be attributed to its uncoated construction and lower fabric density (as in Table II), which facilitates greater airflow through the fabric.

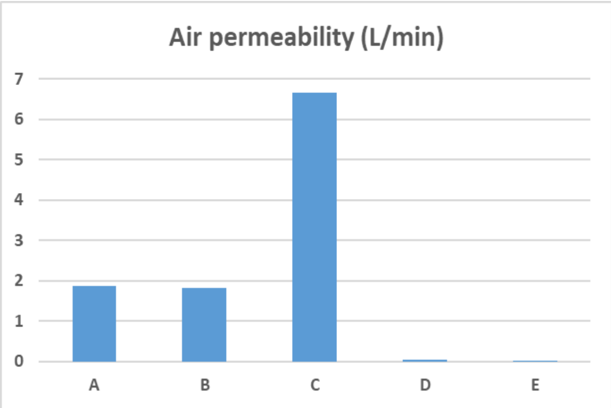

Fig. 3. Air permeability test results

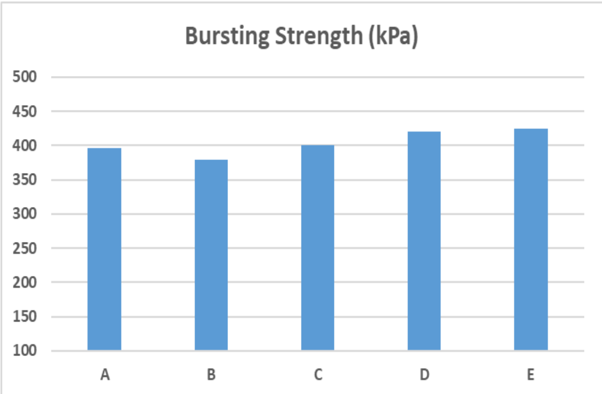

Fig. 4. Bursting strength test result

Fig. 4 illustrates that all five samples exceeded the required bursting strength of 348 kPa. Samples D and E exhibited the highest bursting strength values (~400 kPa), likely due to their ripstop weave structure and higher fabric compactness. Sample B recorded the lowest strength (~380 kPa), but it was still well above the minimum requirement, ensuring sufficient durability for the application.

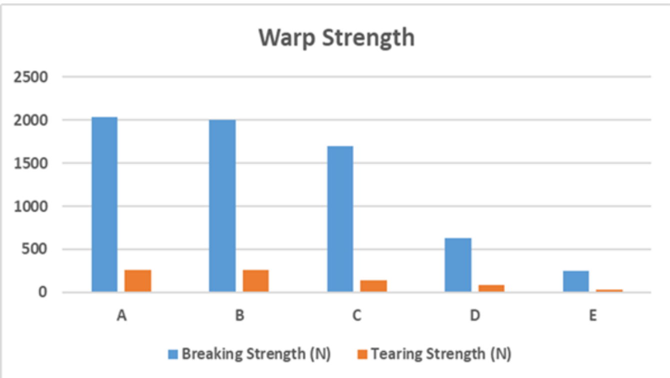

Fig. 5. Warp strength test results

The tensile and breaking strength of the five fabric samples were evaluated in both the weft and warp directions to assess their durability and resistance to mechanical stress. This data is essential to ensure how well the fabric can withstand tension and resist the propagation of tears, especially in high-performance applications.

In the warp direction, as in Fig. 5, a similar performance trend was observed. Samples A and B once again showed superior strength, with breaking strengths of 2038.5 N and 1998.59 N and tearing strengths of 254 N and 262 N, respectively. Their consistent strength in both fabric directions further supports their suitability for high-stress applications. Sample C performed moderately, with a warp-breaking strength of 1702 N and a tearing strength of 139 N, which is in line with its weft directional performance. Conversely, Samples D and E showed significantly lower strength in the warp direction.

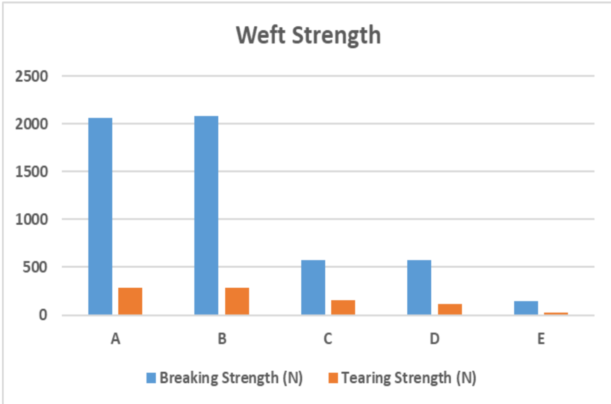

Fig. 6. Weft strength test results

In the weft direction, as in Figure 6, Samples A and B recorded the highest breaking strengths, measuring 2059 N and 2082.03 N, respectively, along with high tearing strengths of 281 N and 290 N. These results reflect the strong structural integrity provided by the coated PA66 fiber and plain weave construction, which contributes to better load distribution across the fabric. Sample C, with a breaking strength of 575.9 N and a tearing strength of 154 N, showed moderate performance, likely due to its uncoated PET fiber content and lower fabric density. On the other hand, Samples D and E exhibited significantly lower weft directional strength.

VI. Conclusion

Skydiving poses a high risk of lower limb injuries, particularly during high-speed landings, which account for many impact-related incidents. Conventional footwear, such as running shoes, provides minimal impact absorption, offering inadequate protection against ground reaction forces that can approach or exceed biomechanical tolerance limits. While innovative solutions like airbag soles and recoil-based military boots have been proposed, their actual effectiveness remains unquantified. This highlights the need for a validated, efficient impact absorption system. Drawing inspiration from automotive airbags, this study proposes the use of a fabric-based air component with controlled air permeability to extend collision time and reduce landing force, offering a promising direction for safer skydiver landings.

The findings of this study demonstrate the importance of selecting a suitable fabric with controlled air permeability for the proposed design. Therefore, five fabric samples were tested, as mentioned below. Samples D and E exhibit air permeability levels below the required threshold, while the other three samples exceed the required air permeability level of 1.6 L/min. Therefore, based on air permeability, fabric samples A, B, and C are initially considered suitable. Since all five samples exhibit similar bursting strength values, this property does not differentiate their performance.

To further assess the durability and mechanical resistance of the fabrics, breaking strength and tearing strength tests were performed. In the warp direction, samples A, B, and C show the highest values. However, in the weft direction, Sample C demonstrates significantly lower strength compared to Samples A and B. Based on both directional strength performance, samples A and B are more appropriate. Among these two, sample A has a slightly higher bursting strength, aligning more closely with the specified requirement. Therefore, Sample A is identified as the most suitable fabric for impact absorption in a skydiver's high-speed landing application.

ACKNOWLEDGMENT

Appreciation is also conveyed to North Sails (Pvt) Ltd for their valuable collaboration in fabric sourcing, which contributed significantly to the quality and success of the outcome.

REFERENCES

[1] "That's How We Roll: Ankle Injuries in Skydiving," United States Parachute Association. Accessed: Oct. 31, 2024. [Online]. Available: https://www.uspa.org/thats-how-we-roll-ankle-injuries-in-skydiving

[2] M. Jong, A. Westman, and B.-I. Saveman, "Experiences of Injuries and Injury Reporting among Swedish Skydivers," *J. Sports Med.*, vol. 2014, p. 102645, 2014, doi: 10.1155/2014/102645.

[3] W. Kong, K. Kasturi, and C. Lee, "Biomechanical modeling of paratrooper landings," in *16th AIAA Aerodynamic Decelerator Systems Technology Conference and Seminar*, Boston,MA,U.S.A.: American Institute of Aeronautics and Astronautics, May 2001. doi: 10.2514/6.2001-2029.

[4] J. W. Whitting, J. R. Steele, M. A. Jaffrey, and B. J. Munro, "Parachute Landing Fall Characteristics at Three Realistic Vertical Descent Velocities," *Aviat. Space Environ. Med.*, vol. 78, no. 12, pp. 1135–1142, Dec. 2007, doi: 10.3357/ASEM.2108.2007.

[5] M. Pal, A. Maity, B. R. Chauhan, H. Juneja, and M. Kumar, "Comparative Analysis of Kinetic Responses and Injury Risk During Landing from 45 cm Height: A Study of Barefoot vs. Sports Shoes Conditions," *Int. J. Phys. Educ. Fit. Sports*, pp. 64–76, Sep. 2024, doi: 10.54392/ijpefs2437.

[6] C. Baoxuan, W. Qingguo, Z. Qiang, M. Haitao, C. Dongan, J. Yuhua, and L. Fangzheng, "A paratrooper shoe sole with automatically inflated airbag," CN2357543Y [Online]. Available: https://patents.google.com/patent/CN2357543Y/en#citedBy

[7] S. Fei, Z. Shu, C. Xinsheng, W. Yongchun, H. Zebing, plateau, and Z. Jiangdong, "High-altitude parachuting and pressure recoil military boot matched surface expanding system and high-altitude inflatable trousers," CN111348195A [Online]. Available: https://patents.google.com/patent/CN111348195A/en?oq=CN111348195A

[8] A. Tagybergen, "Displacement and velocity/ time graphs for the sky diver", Accessed: Feb. 28, 2025. [Online]. Available: https://www.academia.edu/9167147/Displacement_and_velocity_time_graphs_for_the_sky_diver

[9] O. Golubeva and A. Pogorelova, "Analysis of the quality of modern polymer materials of sole," *E3S Web Conf.*, vol. 273, p. 05002, 2021, doi: 10.1051/e3sconf/202127305002.

[10] Q. Zhang, H. Q. Li, Y. K. Ning, D. Liang, and G. R. Zhao, "Design and Realization of a Wearable Hip-Airbag System for Fall Protection," *Appl. Mech. Mater.*, vol. 461, pp. 667–674, Nov. 2013, doi: 10.4028/www.scientific.net/AMM.461.667.

[11] M. Shoaib, A. M. Iqbal, and M. A. Imran, "Measurement of Acceleration Due to Gravity Using Arduino and Ultrasonic Sensor," *J. Sens. Technol.*, vol. 11, no. 04, pp. 55–63, 2021, doi: 10.4236/jst.2021.114004.

[12] A. Sabatini and V. Genovese, "A Sensor Fusion Method for Tracking Vertical Velocity and Height Based on Inertial and Barometric Altimeter Measurements," *Sensors*, vol. 14, no. 8, pp. 13324–13347, Jul. 2014, doi: 10.3390/s140813324.

[13] R. L. Bulathsinghala, S. Fernando, T. S. S. Jayawardana, N. Heenkenda, S. Jeyakumar, P. Packiyarasa, G. Hemamala, and D. Wijesena, "An automatic air inflated tubeless safety jacket for motorbike riders," *Res. J. Text. Appar.*, vol. 26, no. 2, pp. 170–186, Apr. 2022, doi: 10.1108/RJTA-01-2021-0002.

[14] H. Mankodi and B. Kodinaria, "Airjet Textured Yarn Fabrics for Airbag: An Innovative Approach," vol. 10, 2020, doi: 10.37421/jtese.2020.10.423.

[15] R. Nayak, R. Padhye, K. Sinnappoo, L. Arnold, and B. K. Behera, "Airbags," *Text. Prog.*, vol. 45, no. 4, pp. 209–301, Dec. 2013, doi: 10.1080/00405167.2013.859435.